ELSEVIER

Engineering Structures 23 (2001) 790–801

ENGINEERING STRUCTURES

www.elsevier.com/locate/engstruct

A state-space approach for dynamic analysis of sliding structures

Yen-Po Wang *, Wei-Hsin Liao, Chien-Liang Lee

Department of Civil Engineering, National Chiao-Tung University, 1001 Ta Hsueh Road, Hsinchu, Taiwan, ROC

Received 29 August 1999; received in revised form 12 May 2000; accepted 24 July 2000

Abstract

This study presents a numerical algorithm based on a state-space approach for the dynamic analysis of sliding systems. According to the proposed scheme, the equations of motion for the base-isolated structure in both the stick and slip phases are integrated into a single set of equations by treating the friction force as a Lagrange multiplier. The Lagrange multiplier is determined, with additional conditions of equilibrium and kinematic compatibility at the sliding interfaces, via a simple matrix algebraic calculation within the framework of state-space formulations. The responses can thus be obtained recursively from the discrete-time state-space equation using a one-step correction procedure. In addition, the integration step size is maintained constant throughout the analysis. The effectiveness of the proposed scheme is confirmed through examples of sliding systems, under conditions of either free vibration or harmonic excitations, for which analytical solutions are available. Additionally, the novel algorithm is compared with a corrective psuedo-force iterative procedure for seismic response analysis of a FPS-supported five-story building. The novel algorithm is more systematic and easy to implement than conventional approaches. Moreover, by simplifying the task, the proposed algorithm also enhances accuracy and efficiency.

Keywords: State-space; Sliding systems; Dynamic analysis

1. Introduction

Base isolation is a promising approach to protecting civil engineering structures from earthquakes. By implementing isolation devices at the base of the structures, the transmission path of seismic force is released, thus reducing the seismic force applied to the structure significantly. Isolation devices are essentially classified into two types: rubber bearings and sliding bearings. Although rubber bearings have been extensively applied in base isolation systems, sliding bearings have recently found increasing applications [1–3]. Implementing sliding bearings limits the shear force transmitted to the structure to the maximum frictional force of the sliding bearings, regardless of earthquake intensity. If the sliding bearings were frictionless, the transmission path of the seismic force would be completely released, although the sliding displacement could be excessive. Over-displacing of the bearings can be relieved by the friction mechanism of the sliding surfaces dissipating vibration energy. The introduction of friction pendulum systems (FPS) will further enhance the position-restoring and frequency-tuning capability of the isolation system. These characteristics make sliding bearings functionally equivalent to rubber bearings in many applications.

Because the stick and the slip phases exist alternately, depending on the magnitude of the shear forces at the interfaces of the sliding bearings, the dynamic behavior of a sliding structure can be highly nonlinear. This behavior is so complicated that an analytical solution is limited to the harmonic motions of sliding structures with a maximum of two degrees of freedom [4,5]. More realistic transient responses of generic sliding structures can only be obtained numerically. Mostaghel and Tanbakuchi [6] proposed a semi-analytical solution procedure involving alternately using two sets of motion equations corresponding to the stick and slip phases of the system, respectively. Yang et al. [7] proposed a numerical solution procedure based on Newmark's constant-average-acceleration method involving attaching a fictitious spring to the foundation floor, with a stiffness of either zero for slip phases or infinity for stick phases, to represent the frictional effect of the sliding bearings. Moreover, Nagarajaiah et al. [8] proposed a corrective

* Corresponding author. Fax: +886-3-571-3221.
E-mail address: ypwang@cc.nctu.edu.tw (Y.-P. Wang).

0141-0296/01/$ - see front matter
PII: S0141-0296(00)00096-1

pseudo-force iterative procedure, also based on Newmark's method, for the dynamic analysis of three-dimensional base isolated structures, in which the behavior of the friction mechanism is governed by a nonlinear differential equation known as Wen's model [9]. This nonlinear differential equation is solved by a semi-implicit Runge–Kutta method [10]. To ensure the analysis converges with sufficient accuracy, the step size used either has to be kept sufficiently small (for example, $\Delta t \leq 10^{-3}$ s, or an even smaller step size for high-frequency structures) or reduced near the stick–slip transitions (as in [8]), which inevitably makes the solution process rather unwieldy and computationally inefficient.

While Newmark's method is most popular for dynamic analysis of linear or nonlinear systems, the state-space procedure (SSP) is comparably effective in the context of numerical stability and accuracy. The two approaches differ mainly in that Newmark's method is based on the approximation of derivatives (representing the structural responses) of the second-order differential equation, while the SSP method is based on piecewise interpolation of the discrete loading functions so that the convolution integral can be carried out. Since the SSP method enforces no assumption on the response functions, distortion of the dynamic characteristics of the systems is relatively mild compared with Newmark's method. Meanwhile, assessment of the numerical accuracy for both the numerical procedures via a frequency-domain analysis of linear systems indicates that the SSP method is more accurate, as presented in Appendix A.

This study presents a simple and efficient procedure for the dynamic analysis of sliding structures based on a state-space approach [11]. The equations of motion for a base-isolated structure in both the stick and slip phases are integrated into a single set of equations by treating the friction force as a Lagrange multiplier. The Lagrange multiplier can be determined with additional conditions of equilibrium and kinematic compatibility at the sliding interfaces, by simple matrix algebraic calculation within the framework of state-space formulations. The responses can thus be obtained recursively from the discrete-time state-space equation via a one-step correction procedure, and a constant integration time step is used throughout the analysis. Effectiveness of the proposed scheme is verified by analyzing, respectively, a single-degree-of-freedom (SDOF) and two-degree-of-freedom (2DOF) sliding structure for which analytical solutions are available. Additionally, the proposed scheme is compared to a corrective pseudo-force iterative procedure for seismic response analysis of a FPS-supported five-story building. Being more systematic and easy to implement, the proposed algorithm simplifies the task, while also enhancing accuracy and efficiency.

2. Friction mechanism

The motion of the friction bearings can be resolved into stick and slip phases. The stick phase occurs when the vibration-induced shear force between the sliding interfaces of the bearing fails to overcome the maximum friction force. On such an occasion, the relative velocity between the sliding interfaces is zero. However, once the shear force reaches the maximum friction force, the bearing takes no more shear and is forced to slide. The friction force dissipates energy during the slip modes. The friction force, F, acting along the sliding surfaces is governed by

$$|F| \leq \mu W \tag{1}$$

where W is the weight of the structure, and μ is the coefficient of friction which is material-dependent. The frictional coefficient of Teflon–steel interfaces, for example, depends on sliding velocity and bearing pressure, as proposed by Mokha et al. [12,13] as

$$\mu = \mu_{\max} - (\mu_{\max} - \mu_{\min}) \exp(-a|\dot{u}_b|) \tag{2}$$

where $\mu_{\max}$ and $\mu_{\min}$ are the maximum and minimum values of the coefficient of friction, respectively; $\dot{u}_b$ is the sliding velocity of the bearing and coefficient a is determined from bearing pressure. For Coulomb's model [14], the frictional coefficient is assumed to be constant.

In summary, the stick conditions require that

$$|F| < \mu W \tag{3a}$$

and

$$\dot{u}_b = 0 \tag{3b}$$

whereas slip conditions occur only if

$$F = \mu W \operatorname{sgn}(\dot{u}_b) \tag{4a}$$

in which sgn denotes the signum function, and

$$\dot{u}_b \neq 0 \tag{4b}$$

3. Solution algorithm for generic sliding systems

The equation of motion of a generic sliding structure under external disturbances $\mathbf{w}(t)$ can be represented as

$$\mathbf{M}\ddot{\mathbf{u}}(t) + \mathbf{C}\dot{\mathbf{u}}(t) + \mathbf{K}\mathbf{u}(t) = \mathbf{E}\mathbf{w}(t) + \mathbf{B}F(t) \tag{5}$$

where $\mathbf{u}(t)$ is the $n \times 1$ displacement vector, $\mathbf{M}$, $\mathbf{C}$, $\mathbf{K}$ are respectively the $n \times n$ mass, damping and stiffness matrices, $\mathbf{E}$ is the $n \times q$ location matrix of the external loads, $\mathbf{w}(t)$ is the $q \times 1$ loading vector, $\mathbf{B}$ is the $n \times 1$ location matrix of the friction force and $F(t)$ is the friction force satisfying conditions described in Eqs. (3a) and (3b), or Eqs. (4a) and (4b).

3.1. State-space representation

Eq. (5) can be represented in a state-space representation, leading to a first-order differential equation as [11]

$$\dot{\mathbf{z}}(t)=\mathbf{A}^*\mathbf{z}(t)+\mathbf{E}^*\mathbf{w}(t)+\mathbf{B}^*F(t) \tag{6}$$

where

$$\mathbf{z}(t)=\begin{bmatrix}\mathbf{u}(t)\\ \dot{\mathbf{u}}(t)\end{bmatrix}$$

is the $2n\times1$ state vector,

$$\mathbf{A}^*=\begin{bmatrix}\mathbf{0} & \mathbf{I}\\ -\mathbf{M}^{-1}\mathbf{K} & -\mathbf{M}^{-1}\mathbf{C}\end{bmatrix}$$

is the $2n\times2n$ system matrix,

$$\mathbf{B}^*=\begin{bmatrix}\mathbf{0}\\ \mathbf{M}^{-1}\mathbf{B}\end{bmatrix}$$

is the $2n\times1$ friction loading matrix, and

$$\mathbf{E}^*=\begin{bmatrix}\mathbf{0}\\ \mathbf{M}^{-1}\mathbf{E}\end{bmatrix}$$

is the $2n\times q$ external loading matrix.

With first-order interpolations of the loading terms between two consecutive sampling instants, the state Eq. (6) can further be resolved as a difference equation to be [11]

$$\mathbf{z}[k]=\mathbf{A}\mathbf{z}[k-1]+\mathbf{B}_0F[k-1]+\mathbf{B}_1F[k]+\mathbf{E}_0\mathbf{w}[k-1]+\mathbf{E}_1\mathbf{w}[k] \tag{7}$$

where $\mathbf{A}=e^{\mathbf{A}^*\Delta t}$ is the $2n\times2n$ discrete-time system matrix with Δt being the integration time step,

$$\mathbf{B}_0=\left[(\mathbf{A}^*)^{-1}\mathbf{A}+\frac{1}{\Delta t}(\mathbf{A}^*)^{-2}(\mathbf{I}-\mathbf{A})\right]\mathbf{B}^*$$

is the $2n\times1$ discrete-time friction loading matrix of the previous time step,

$$\mathbf{B}_1=\left[-(\mathbf{A}^*)^{-1}+\frac{1}{\Delta t}(\mathbf{A}^*)^{-2}(\mathbf{A}-\mathbf{I})\right]\mathbf{B}^*$$

is the $2n\times1$ discrete-time friction loading matrix of the current time step,

$$\mathbf{E}_0=\left[(\mathbf{A}^*)^{-1}\mathbf{A}+\frac{1}{\Delta t}(\mathbf{A}^*)^{-2}(\mathbf{I}-\mathbf{A})\right]\mathbf{E}^*$$

is the $2n\times q$ discrete-time external loading matrix of the previous time step, and

$$\mathbf{E}_1=\left[-(\mathbf{A}^*)^{-1}\mathbf{A}+\frac{1}{\Delta t}(\mathbf{A}^*)^{-2}(\mathbf{A}-\mathbf{I})\right]\mathbf{E}^*$$

is the $2n\times q$ discrete-time external loading matrix of the current time step.

3.2. Shear-balance procedure (SBP)

The discrete-time state-space equation (7) reveals that, the friction force, $F[k]$, of the current time instant depends on the motion conditions, which are not known as a priori. Therefore, the solution cannot be obtained directly through simple recursive calculations. Rather than using an iterative corrective pseudo-force procedure as is common for nonlinear dynamic analysis, a procedure based on the concept of shear balance at the sliding interfaces is proposed.

As the friction mechanism reveals, the base shear force and sliding velocity of the base floor are indicators of the motion conditions. During the slip phases, the friction force is defined by Eq. (4a), but the sliding velocity remains unknown. Meanwhile, during the stick phases, the sliding velocity at the base floor is zero, as defined by Eq. (3b), but the friction force (or equivalently, the base shear) remains undetermined. Restated, either the friction force or sliding velocity is known, depending on the motion condition. This extra condition allows the base shear, $F[k]$, to be uniquely determined at time instant k.

Initially, for time instant k, granting a stick condition for the system gives

$$\dot{u}_b[k]=\mathbf{D}\mathbf{z}[k]=0 \tag{8}$$

where $\mathbf{D}=[\mathbf{0}\ \ \mathbf{B}^T]$ is the $2n\times1$ location vector of the base velocity $\dot{u}_b[k]$. Substituting Eq. (7) for $\mathbf{z}[k]$ in Eq. (8), the base shear force, $\bar{F}[k]$, that would prevent the system from sliding, can be resolved in a closed-form as

$$\bar{F}[k]=-(\mathbf{D}\mathbf{B}_1)^{-1}\mathbf{D}(\mathbf{A}\mathbf{z}[k-1]+\mathbf{E}_0\mathbf{w}[k-1]+\mathbf{E}_1\mathbf{w}[k]+\mathbf{B}_0F[k-1]) \tag{9}$$

which, according to the friction law, should be below the maximum friction force.

Now, if $|\bar{F}[k]|<\mu W$, then the stick condition granted initially in the analysis is correct, and the actual friction force is updated as $F[k]=\bar{F}[k]$; otherwise, the system should be in the slip phase instead, and the friction force is corrected accordingly as $F[k]=\mu W\,\mathrm{sgn}(\bar{F}[k])$. With $F[k]$ determined, the response, $\mathbf{z}[k]$, of the isolated system can be obtained from Eq. (7).

When a more sophisticated friction mechanism is considered, the solution requires an iterative procedure to locate the corresponding friction coefficient during sliding. For example, taking Mokha's model, where the frictional coefficient depends on the sliding velocity, $\dot{u}_b[k]$, as described by Eq. (2), the procedure is revised as:

1. Calculate the friction force, $\bar{F}[k]$, by Eq. (9).
2. If $|\bar{F}[k]|<\mu_{\min}W$, then the granted stick condition is

correct. The actual friction force is revised as $F[k]=\bar{F}[k]$; otherwise, the system should be in a slip phase instead, and the friction force is corrected in accordance with $F[k]=\mu W \operatorname{sgn}(\bar{F}[k])$.

3. Calculate system response $\mathbf{z}[k]$, by Eq. (7).
4. Determine the coefficient of friction, $\bar{\mu}$, by Eq. (2) corresponding to the sliding velocity $\dot{u}_b=\mathbf{Dz}[k]$ obtained in step 3.
5. If $|(\bar{\mu}-\mu)/\mu|\geq$err where err is the allowable error, set $F[k]=-\bar{\mu}W \operatorname{sgn}(\dot{u}_b[k])$ and $\mu=\bar{\mu}$, then return to step 2; otherwise, the solution is accepted, so proceed to the next time step.

4. Numerical verifications

4.1. Free-vibration response of SDOF sliding systems with Coulomb friction

The proposed numerical scheme is first applied to solve the free-vibration response of a Coulomb-friction-damped sliding system, illustrated in Fig. 1. The equation of motion of this system can be expressed as [14]

$$\ddot{u}+\omega_n^2 u=-\mu g \operatorname{sgn}(\dot{u}) \tag{10}$$

where ω_n is the natural frequency of the system and g is the gravitational acceleration. Given initial displacement $u(0)=U_0$, the free vibration response of the system, normalized with respect to U_0, is readily obtained in a closed-form solution as

$$\frac{u(t/T_n)}{U_0}=\left[1-(2j-1)\frac{\mu g}{U_0\omega_n^2}\right]\cos\left(2\pi\frac{t}{T_n}\right)- \tag{11}$$

$$(-1)^j\frac{\mu g}{U_0\omega_n^2},\ \frac{j-i}{2}\leq\frac{t}{T_n}\leq\frac{j}{2}$$

where T_n is the fundamental period of the sliding system, $j=1, 2, \ldots$ but

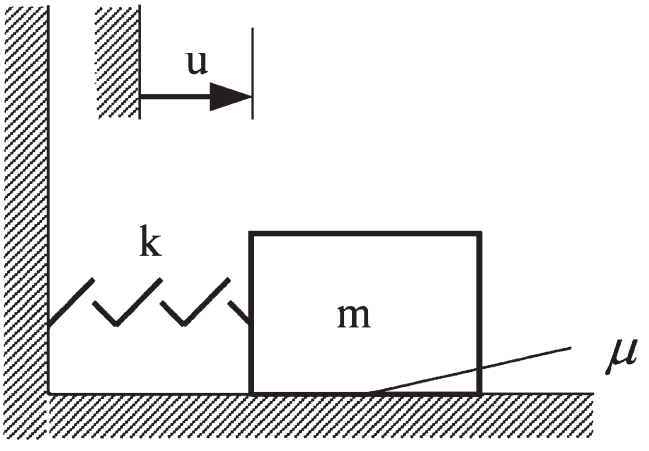

Fig. 1. Coulomb-friction-damped sliding system.

$$j\leq\frac{U_0\omega_n^2}{2\mu g} \tag{12}$$

The above inequality can be derived from the equilibrium. Notably, the motion ceases when $j>(U_0\omega_n^2)/2\mu g$. Furthermore, the spring–mass sliding system will return to an undeformed position when the oscillation stops if $U_0\omega_n^2/2\mu g$ is an integer, otherwise the mass will be permanently offset from its origin

Fig. 2 illustrates the free vibration responses, in terms of displacement, acceleration and friction force, for $U_0\omega_n^2/2\mu g=10$, considering the sampling ratio, $\Delta t/T_n$, of 0.1 and 0.01, respectively. For $\Delta t/T_n=0.1$, significant discrepancies exist between numerical (SBP) and analytical solutions, especially when the motion ceases after five cycles of free oscillation (as predicted by inequality (12)) where the estimated friction is seriously distorted. The error arises mainly from assuming a linear variation of the friction force between two consecutive sampling points in the analysis, an assumption which is not valid during stick–slip transitions or direction switches when both the acceleration and friction responses are discontinuous. However, the error becomes insignificant as the sampling ratio, $\Delta t/T_n$, decreases to 0.01. Numerical results closely match the analytical solutions even during

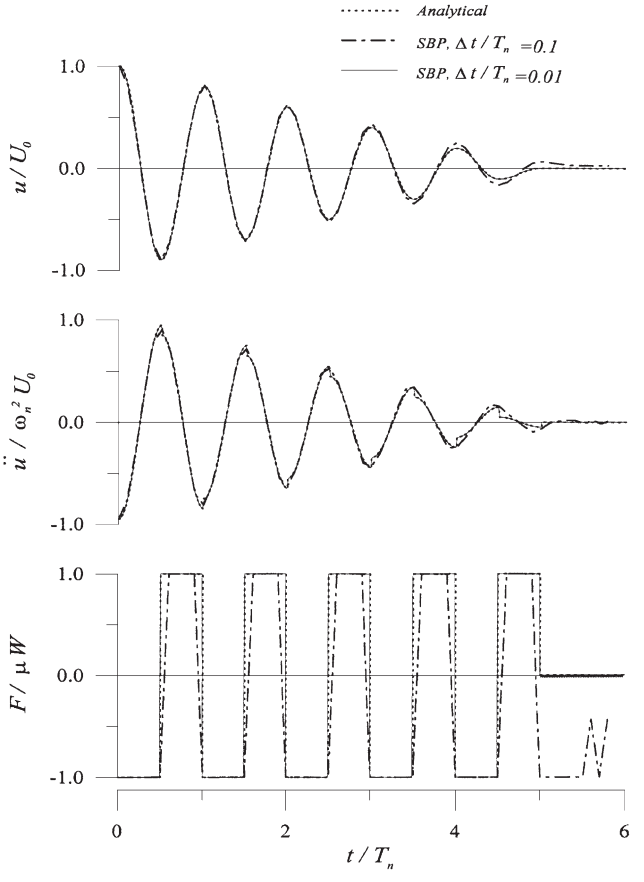

Fig. 2. Free vibration of the SDOF Coulomb-friction-damped system ($\omega_n^2U_0/2\mu g=10$).

phase transitions. A sampling ratio of 0.01, which is comparatively large for nonlinear dynamic analysis, is considered sufficient.

Fig. 3 further illustrates the corresponding results for $U_0\omega_n^2/2\mu g$=2.3. While the predicted displacement response closely approximates the analytical displacement for $\Delta t/T_n$=0.01, acceleration and friction are only accurate during the sliding phase. In the stick phase, following one cycle of free oscillation, the numerical prediction does not converge to the analytical solution, even with a reduced sampling ratio. Nevertheless, the numerical solution is not divergent either, indicating no error accumulation.

4.2. Harmonic response of a 2DOF sliding system

The response of sliding structures to harmonic support motion, studied by Mostaghel et al. [5] via a semi-analytical procedure, is further investigated herein. Fig. 4 shows a single-story structure of mass m, damping c and stiffness k, supported by a foundation raft of mass M that can slide horizontally. The Coulomb frictional coefficient is μ. When the ground moves with acceleration $\ddot{x}_0$, the dynamic response of the system is governed by

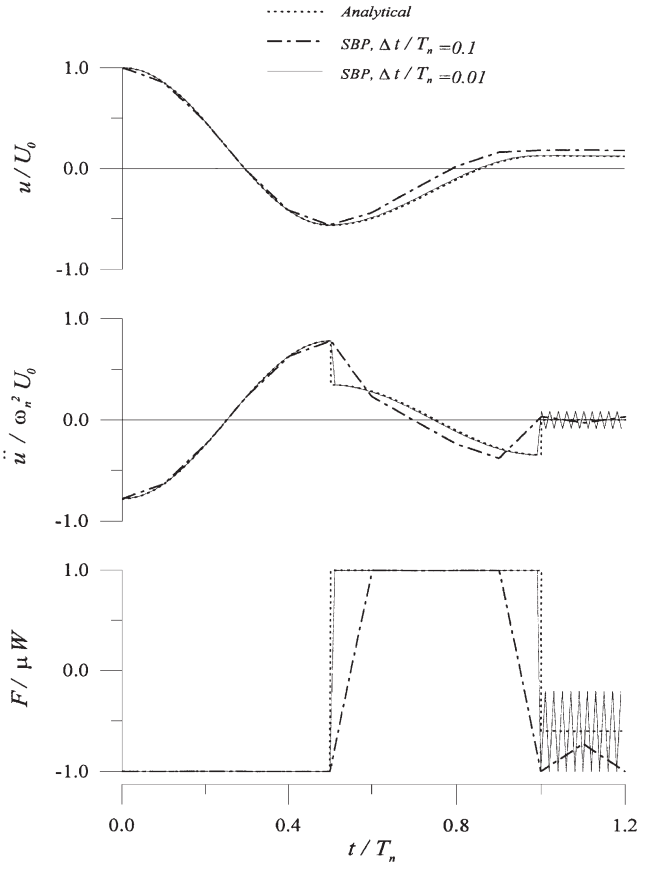

Fig. 3. Free vibration of the SDOF Coulomb-friction-damped system ($\omega_n^2U_0/2\mu g$=2.3).

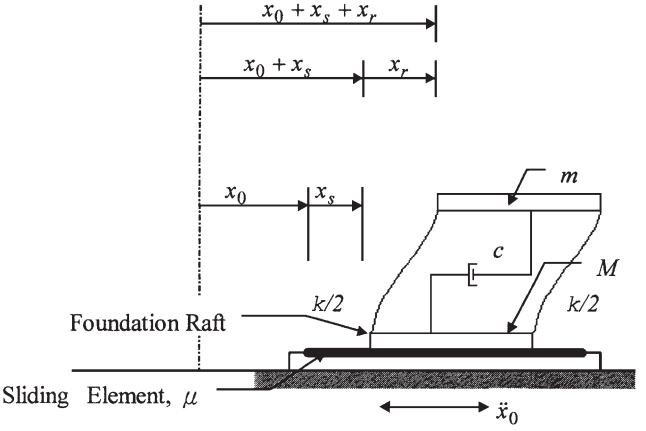

Fig. 4. Single-story structure on sliding support.

$$\begin{bmatrix} m & m \\ m & M+m \end{bmatrix}\begin{pmatrix} \ddot{x}_r \\ \ddot{x}_s \end{pmatrix}+\begin{bmatrix} c & 0 \\ 0 & 0 \end{bmatrix}\begin{pmatrix} \dot{x}_r \\ \dot{x}_s \end{pmatrix}+\begin{bmatrix} k & 0 \\ 0 & 0 \end{bmatrix}\begin{pmatrix} x_r \\ x_s \end{pmatrix}= -\begin{pmatrix} m \\ M+m \end{pmatrix}\ddot{x}_0+\begin{pmatrix} 0 \\ F \end{pmatrix} \tag{13}$$

where x_r is the story displacement relative to the foundation raft, x_s is the sliding displacement of the foundation relative to the ground, and F is the friction force. When the foundation raft slides, the friction force satisfies

$$F=-\mu g(m+M)\,\mathrm{sgn}(\dot{x}_s) \tag{14}$$

Without losing the generality, Eq. (13) can be more conveniently expressed as

$$\begin{bmatrix} 1 & 1 \\ \alpha & 1 \end{bmatrix}\begin{pmatrix} \ddot{x}_r \\ \ddot{x}_s \end{pmatrix}+\begin{bmatrix} 2\zeta\omega_n & 0 \\ 0 & 0 \end{bmatrix}\begin{pmatrix} \dot{x}_r \\ \dot{x}_s \end{pmatrix}+\begin{bmatrix} \omega_n^2 & 0 \\ 0 & 0 \end{bmatrix}\begin{pmatrix} x_r \\ x_s \end{pmatrix}= -\begin{pmatrix} 1 \\ 1 \end{pmatrix}\ddot{x}_0-\begin{pmatrix} 0 \\ \alpha F/m \end{pmatrix} \tag{15}$$

where $\alpha=m/(M+m)$, $\omega_n=\sqrt{k/m}$ and $\zeta=c/(2m\omega_n)$.

A series of parametric studies has been conducted following Mostaghel et al. [5] for the sake of comparison. These studies considered harmonic support excitation of $\ddot{x}_0=A\sin\Omega t$ with an excitation period of $T_g=2\pi/\Omega$=0.5 s and duration of excitation of 5 s. Response spectra for the absolute accelerations and sliding displacements normalized with respect to the peak ground acceleration, A, and the steady-state peak ground displacement, $D=A/\Omega^2$, are obtained for coefficients of friction μ=0.05, 0.10, 0.15, 0.20, for excitation amplitudes A=0.5 g, and for mass ratios α=0.25, 0.50. The damping ratio is assumed to be 5% of the critical damping, while all calculations use an integration step size of 0.005 s.

Figs. 5(a) and 6(a) show, respectively, the normalized spectral acceleration of structures with mass ratios α=0.25 and 0.5. The responses of the isolated structures are smaller than those of fixed-base structures. Mean-

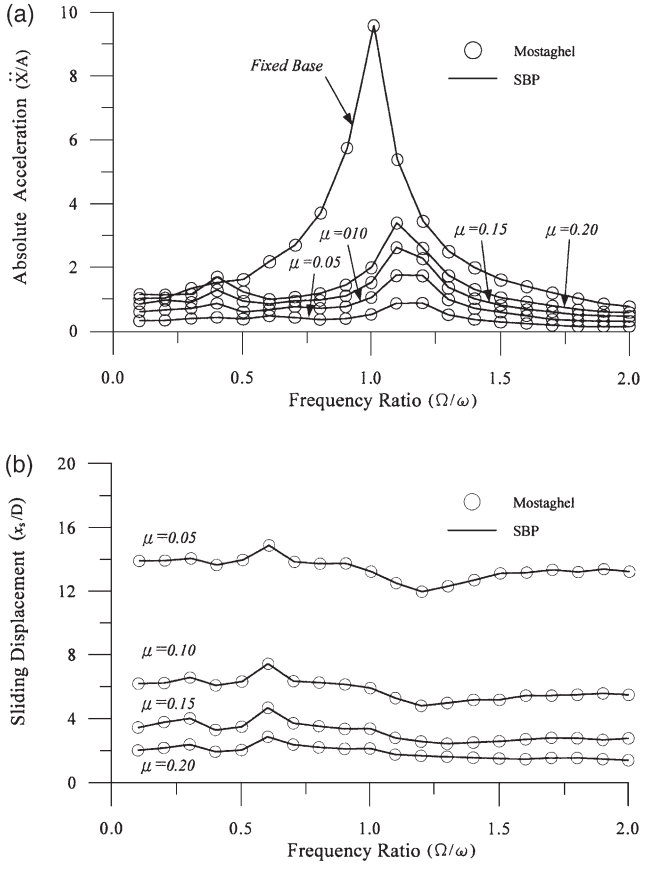

Fig. 5. (a) Variations of acceleration with frequency ratio; (b) variations of sliding displacement with frequency ratio (ξ=5%, α=0.25, A=0.5g, T_g=0.5 s).

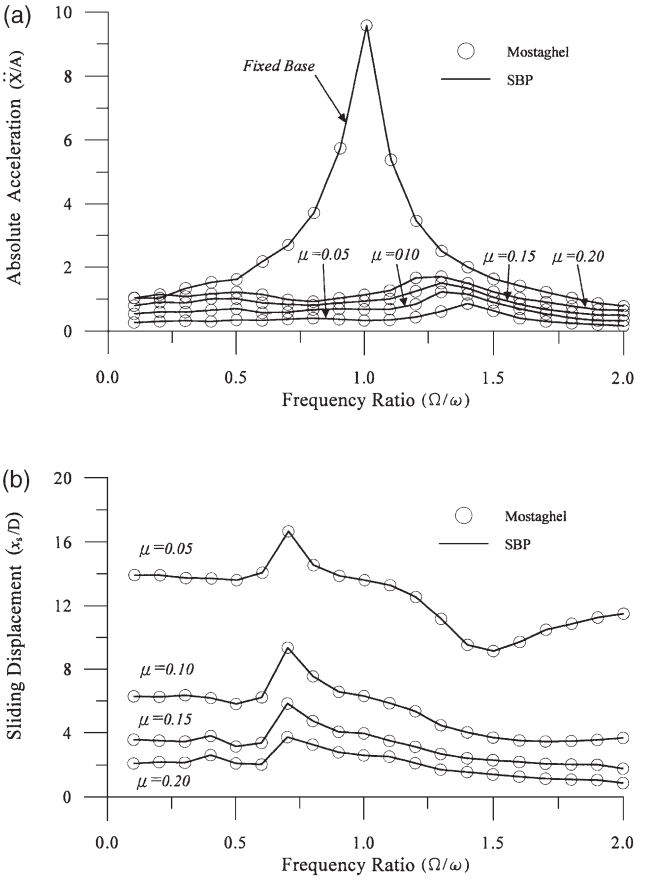

Fig. 6. (a) Variations of acceleration with frequency ratio; (b) variations of sliding displacement with frequency ratio (ξ=5%, α=0.5, A=0.5g, T_g=0.5 s).

while, the responses decrease with declining frictional coefficient. Figs. 5(b) and 6(b) illustrate, respectively, the normalized spectral displacement of sliding for mass ratios α=0.25 and 0.5. The structure slides further with a smaller frictional coefficient. Additionally, the spectral displacements do not vary significantly with frequency ratio when a=0.25. As the mass ratio increases to α=0.5, the spectral displacements become somewhat frequency dependent. Excellent agreement has been observed between the numerical results and the analytical solution by Mostaghel et al., further confirming the effectiveness of the proposed numerical procedure.

4.3. Earthquake response of a five-story base-isolated structure

Finally, the earthquake response analysis of a prototype five-story building implemented with friction pendulum seismic isolation bearings (FPS) is investigated using both the presented SBP method and the corrective pseudo-force iterative procedure (CPIP) by Nagarajaiah et al. [8].

In the CPIP method, the friction force is further represented by Wen's model [9] as

$$F=\mu Wq \tag{16}$$

where μ is the friction coefficient, W is the weight of the structure and q is governed by a nonlinear differential equation as

$$\dot{q}=\eta\dot{x}_s-\beta|\dot{x}_s||q|^{n-1}q-\gamma\dot{x}_s|q|^n \tag{17}$$

where η, β, γ and n are parameters characterizing the hysteresis loops of the friction. To facilitate analysis, these parameters must be carefully calibrated for a prescribed hysteresis obtained by a component test of the isolation bearing. The friction mechanism of Mokha depicted by Eq. (2) is adopted with μ_{max}=0.05, μ_{min}=0.036 and a=78.7 s/m (2 s/in) assumed in this example.

With no analytical solution available, the "exact" hysteresis of a sliding bearing subjected to a harmonic excitation of 0.5 Hz for 30 s is illustrated in Fig. 7(a), which was simulated by the SBP method with Δt=0.0001 s following Mokha's friction mechanism. Employing the SBP method with Δt=0.001 s, prediction of the hysteresis is perfect (Fig. 7(b)), while the calculation is 107 times faster than that required by the "exact" solution in CPU time. When the step size further increases to 0.01

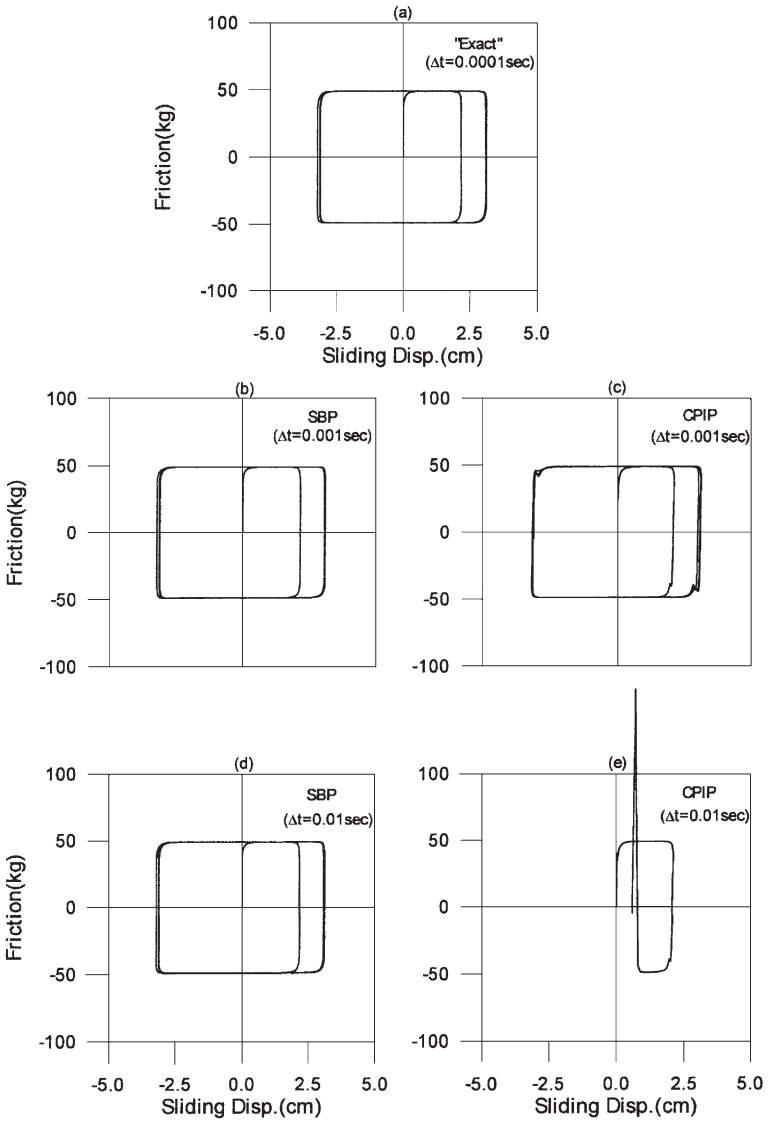

Fig. 7. Hysteresis of friction force under harmonic motion.

s, correlation of the result with the "exact" one is still excellent (Fig. 7(d)), while the calculation is 8369 times faster than that required by the "exact" solution. On the other hand, the parameters of Wen's model in Eq. (17) are determined from a preliminary parametric study to be η=30, β=15, γ=15, and n=2. Employing the CPIP method with Δt=0.001 s, the simulated hysteresis approximates the "exact" one closely, except at the corners where reversing of sliding occurs (Fig. 7(c)), and the calculation is 89 times faster than that required by the "exact" solution. However, the numerical solution diverges when the step size further increases to 0.01 s (Fig. 7(d)).

The seismic response of a five-story model structure with FPS isolators is examined next. The radius of curvature of the FPS bearing is 1 m so that the vibration period of the isolated structure during sliding is shifted to 2 s. The system parameters of the structure are summarized in Appendix B. The 1940 El Centro earthquake is used as the excitation.

Fig. 8 illustrates the hysteresis of friction force. The "exact" solution in Fig. 8(a) is obtained by employing the SBP method with Δt=0.0001 s, since there is no analytical solution available. The results in Fig. 8(b,d) indicate the SPB method with Δt=0.001 or even 0.01 s can sufficiently predict the "exact" hysteresis. Employing the CPIP method, with the same parameters of Wen's model calibrated in the harmonic case, the prediction of the hysteresis with Δt=0.001 s correlates well with the "exact" solution with only small discrepancies (Fig. 8(c)). However, the numerical result diverges when Δt=0.01 s. Fig. 9 illustrates the time history of the sliding displacement. The residual displacement after the earthquake episode is found to be insignificant, indicating a good restoring capability of the FPS isolation system. Clearly, the results by the SBP method with Δt=0.001

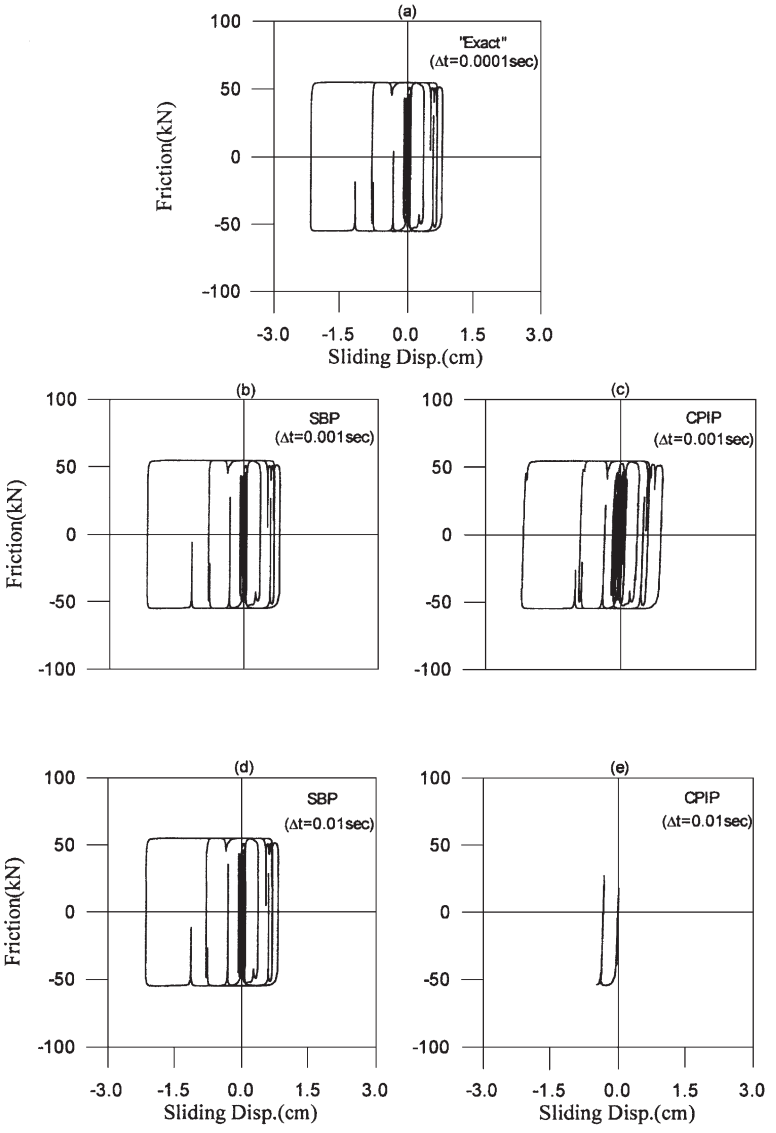

Fig. 8. Hysteresis of friction force under the El Centro earthquake.

and 0.01 s coincide with the "exact" solution, while that by the CPIP with Δt=0.001 s deviates slightly from the "exact" solution. The responses of the roof displacement (relative to the base) reveal a similar trend, as depicted in Fig. 10. Besides, for an acceptable numerical accuracy, the computational time required by the SBP method with Δt=0.01 s is approximately 94 times faster than that required by the CPIP method with Δt=0.001 s, without counting the time needed to calibrate Wen's model. Furthermore, the structural response amplitude, illustrated in Fig. 11, is substantially reduced compared with that without seismic isolation (fixed), confirming the effectiveness of FPS isolation bearings under the El Centro earthquake.

5. Conclusions

This study has developed a numerical procedure based on a state-space difference equation and the concept of shear balance, with additional conditions of equilibrium and kinematic compatibility at the sliding interfaces for the dynamic analysis of sliding structures. Effectiveness of the algorithm is verified through examples of sliding systems, under conditions of either free vibration or harmonic excitations, for which analytical solutions are available. The proposed scheme accurately predicts the nonlinear behavior for forced vibration cases and free vibration cases with $U_0\omega_n^2/2\mu g$ being an integer. However, for free vibration cases with $U_0\omega_n^2/2\mu g$ being a non-integer, the acceleration and friction responses are only

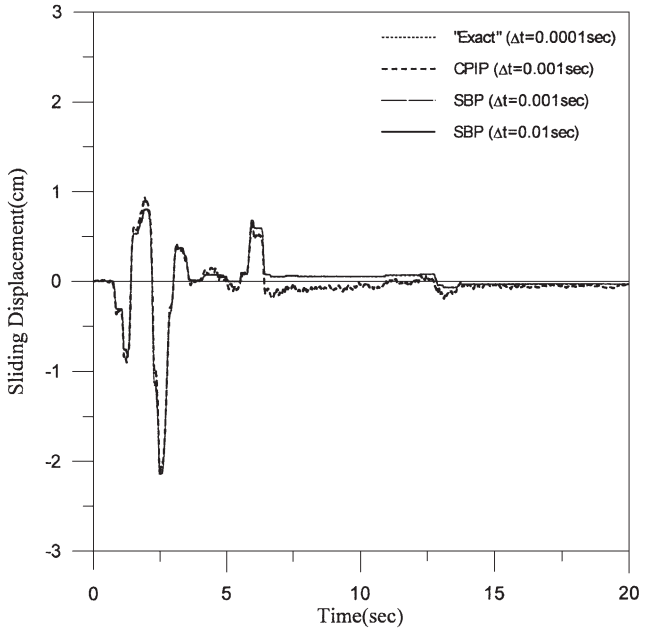

Fig. 9. Sliding displacement of the isolated structure under the El Centro earthquake.

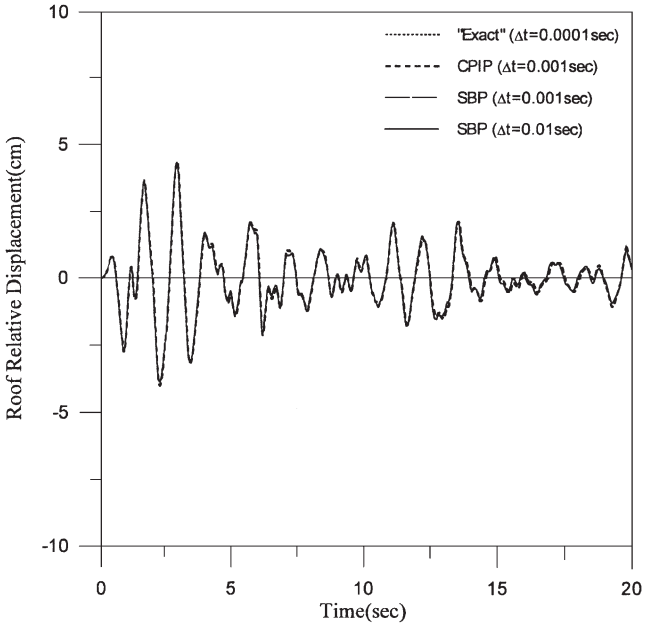

Fig. 10. Roof relative displacement under the El Centro earthquake.

accurate during the sliding phases. Both the proposed scheme and a corrective pseudo-force iterative procedure are applied comparatively for seismic response analysis of a FPS-supported five-story building. Logically simple and easy to implement, the proposed scheme substantially simplifies the task with accuracy and efficiency enhanced to a large extent. The proposed scheme has the following features:

1. The dynamics of the sliding system is represented by a single set of state-space equations without changing any system parameter during the analysis, regardless of either the slip or stick phase.
2. No prescribed hysteresis of friction force is needed, as required by the corrective pseudo-force iterative procedure. The friction force (or Lagrange multiplier) can be obtained by simple matrix algebraic calculation.
3. A constant and relatively larger integration interval is allowed throughout the analysis, compared with the CPIP method. The numerical results that employ the proposed SBP method converge to the "exact" solutions with a step size as large as 0.01 s, thus helping to significantly reduce the computational effort.
4. It requires only a one-step correction without iteration when the Coulomb's model is considered as the friction mechanism. With a moderate modification, the numerical scheme can further resolve problems involving a more sophisticated frictional mechanism such as the Mokha's model.
5. With the friction force(s) treated as an independent variable (vector), this algorithm is flexible enough to be extended further for solving dynamic problems of sliding structures with unsynchronized multiple support motions.

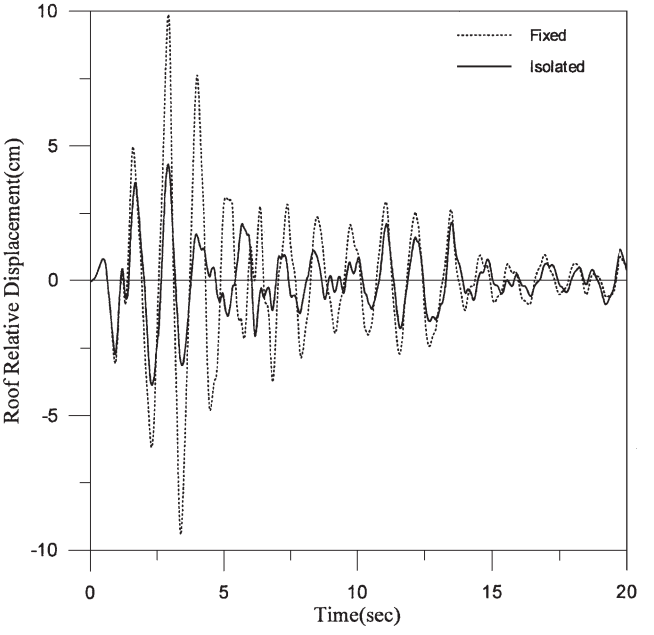

Fig. 11. Roof displacement with and without seismic isolation.

Acknowledgements

This research is sponsored by the National Science Council of the Republic of China under grant no. NSC 88-2625-2009-001. The authors would also like to thank

Dr L.L. Chung, National Center for Research on Earthquake Engineering, Taiwan, for his valuable discussions.

Appendix A

Without a loss of generality, a SDOF structure is considered to investigate the numerical accuracy for both the Newmark and SSP methods.

A.1. Newmark method

The basic equations of the Newmark method are generally formulated as

$$m\ddot{x}[k]+c\dot{x}[k]+kx[k]=-mw[k] \tag{A1}$$

$$x[k]=x[k-1]+\Delta t\dot{x}[k-1]+\Delta t^2\left[\left(\tfrac{1}{2}-\alpha\right)\ddot{x}[k-1]+\alpha\ddot{x}[k]\right] \tag{A2}$$

$$\dot{x}[k]=\dot{x}[k-1]+\Delta t[(1-\delta)\ddot{x}[k-1]+\delta\ddot{x}[k]] \tag{A3}$$

where $x[k]$ is the displacement at the kth time instant, m, c and k are, respectively, the mass, damping and stiffness of the system, w is the ground excitation, Δt is the integration time interval, α and δ are parameters characterizing the approximation strategy. If $\delta\geq 1/2$ and $\alpha\geq\delta/2$, the Newmark method is unconditionally stable.

Eqs. (A1)–(A3) can be concisely expressed in a recursive matrix form as

$$\mathbf{z}[k]=\mathbf{A}\mathbf{z}[k-1]+\mathbf{E}w[k] \tag{A4}$$

where

$$\mathbf{z}[k]=\begin{bmatrix}x[k]\\ \dot{x}[k]\\ \ddot{x}[k]\end{bmatrix}$$

is a 3×1 structural response vector,

$$\mathbf{A}=\begin{bmatrix}1-\Delta t^2\alpha\frac{k}{\hat{m}} & \Delta t-\Delta t^2\alpha\frac{c}{\hat{m}}-\Delta t^3\alpha\frac{k}{\hat{m}} & \Delta t^2\left(\frac{1}{2}-\alpha\right)-\Delta t^3(1-\delta)\alpha\frac{c}{\hat{m}}-\Delta t^4\left(\frac{1}{2}-\alpha\right)\alpha\frac{k}{\hat{m}}\\ -\Delta t\delta\frac{k}{\hat{m}} & 1-\Delta t\delta\frac{c}{\hat{m}}-\Delta t^2\delta\frac{k}{\hat{m}} & \Delta t(1-\delta)-\Delta t^2(1-\delta)\delta\frac{c}{\hat{m}}-\Delta t^3\left(\frac{1}{2}-\alpha\right)\delta\frac{k}{\hat{m}}\\ -\frac{k}{\hat{m}} & -\frac{c}{\hat{m}}-\Delta t\frac{k}{\hat{m}} & -\Delta t(1-\delta)\frac{c}{\hat{m}}-\Delta t^2\left(\frac{1}{2}-\alpha\right)\frac{k}{\hat{m}}\end{bmatrix}$$

is a 3×3 effective system matrix,

$$\mathbf{E}=\begin{bmatrix}-\Delta t^2\alpha\frac{m}{\hat{m}}\\ -\Delta t\delta\frac{m}{\hat{m}}\\ -\frac{m}{\hat{m}}\end{bmatrix}$$

is a 3×1 effective load vector, and $\hat{m}=m+\Delta t\delta c+\Delta t^2\alpha k$ is the effective mass.

Taking a z-transformation of the difference equation

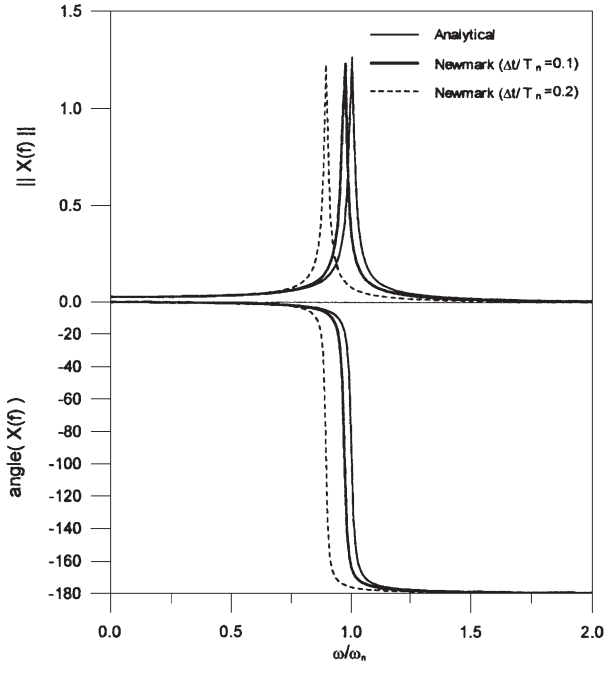

Fig. A1. Frequency response function by the Newmark method (δ=1/2, α=1/4, ξ=0.01).

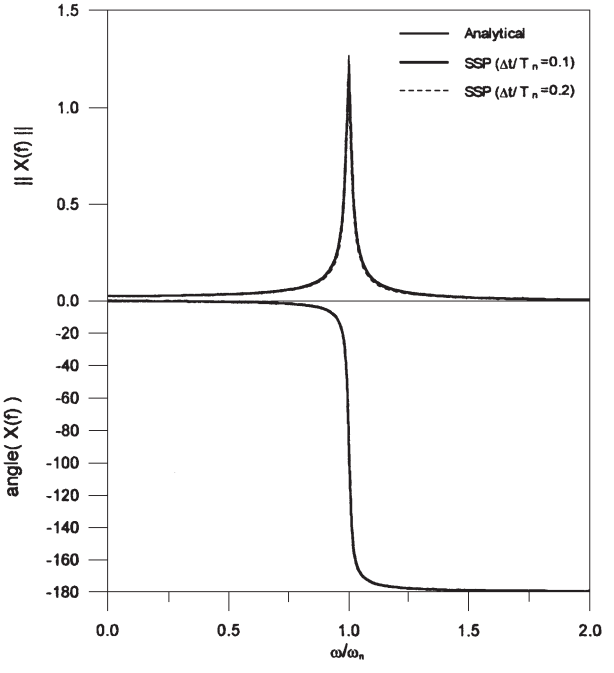

Fig. A2. Frequency response function by the SSP method (ξ=0.01).

Eq. (A4), the structural response $\mathbf{z}[k]$ and the external disturbance $w[k]$ are related in frequency-domain by

$$\mathbf{Z}(z)=\mathbf{H}(z)W(z) \tag{A5}$$

where $\mathbf{Z}(z)$ and $W(z)$ are the z-transforms of $\mathbf{z}[k]$ and $w[k]$, respectively. $\mathbf{H}(z)=(\mathbf{I}-z^{-1}\mathbf{A})^{-1}\mathbf{E}$ is the 3×1 frequency response function by assigning $z=e^{j2\pi f\Delta t}$. The displacement frequency response function, $X(f)$, can be specifically calculated as

$$X(f)=\mathbf{D}(\mathbf{I}-e^{-j2\pi f\Delta t}\mathbf{A})^{-1}\mathbf{E} \tag{A6}$$

where $\mathbf{D}=[1\ 0\ 0]$ is the location vector of the displacement.

A.2. State-space procedure (SSP)

The discrete-time state-space equation of a SDOF structure subjected to ground excitation can be expressed as

$$\mathbf{z}[k]=\mathbf{A}\mathbf{z}[k-1]+\mathbf{E}_0 w[k-1]+\mathbf{E}_1 w[k] \tag{A7}$$

where $\mathbf{A}=e^{\mathbf{A}^*\Delta t}$ is a 2×2 discrete-time system matrix, in which

$$\mathbf{A}^*=\begin{bmatrix} 0 & 1 \\ -\dfrac{k}{m} & -\dfrac{c}{m} \end{bmatrix}$$

$\mathbf{E}_0$ is a 2×1 load matrix of the previous time-step, and $\mathbf{E}_1$ is a 2×1 load matrix of the current time-step. The SSP method is uncondionally stable if the structure itself is stable (that is, $\omega_n>0$ and $\xi>0$), regardless of the step size.

Taking a z-transform of the difference equation (A7), the structural responses $\mathbf{z}[k]$ and the external disturbance $w[k]$ are related in the frequency-domain by

$$\mathbf{Z}(z)=\mathbf{H}(z)W(z) \tag{A8}$$

where $\mathbf{Z}(z)$ and $W(z)$ are the z-transforms of $\mathbf{z}[k]$ and $w[k]$, respectively.

$$\mathbf{H}(z)=(\mathbf{I}-z^{-1}\mathbf{A})^{-1}(z^{-1}\mathbf{E}_0+\mathbf{E}_1)$$

is the 2×1 frequency response function by assigning $z=e^{j2\pi f\Delta t}$. The displacement frequency response function, $X(f)$, can be specifically calculated as

Table 1

System parameter	Parameter value
Mass matrix **M** (N s²/m)	$\begin{bmatrix} 0.1865 & 0 & 0 & 0 & 0 & 0.1865 \\ 0 & 0.1865 & 0 & 0 & 0 & 0.1865 \\ 0 & 0 & 0.1865 & 0 & 0 & 0.1865 \\ 0 & 0 & 0 & 0.1865 & 0 & 0.1865 \\ 0 & 0 & 0 & 0 & 0.1865 & 0.1865 \\ 0.1865 & 0.1865 & 0.1865 & 0.1865 & 0.1865 & 1.1188 \end{bmatrix} *10^5$
Stiffness matrix **K** (N/m)	$\begin{bmatrix} 6.1373 & -3.6755 & 1.1792 & -0.2449 & 0.0382 & 0 \\ -3.6755 & 5.0582 & -3.4378 & 1.0969 & -0.1710 & 0 \\ 1.1792 & -3.4378 & 4.9759 & -3.2733 & 0.7974 & 0 \\ -0.2449 & 1.0969 & -3.2733 & 4.2541 & -1.8829 & 0 \\ 0.0382 & -0.1710 & 0.7974 & -1.8829 & 1.2260 & 0 \\ 0 & 0 & 0 & 0 & 0 & 0.1096 \end{bmatrix} *10^7$
Damping matrix **C** (N s/m)	$\begin{bmatrix} 1.0482 & -0.6020 & 0.2162 & -0.0397 & -0.0081 & 0 \\ -0.6020 & 0.8965 & -0.5467 & 0.1912 & -0.0554 & 0 \\ 0.2162 & -0.5467 & 0.8744 & -0.5428 & 0.1217 & 0 \\ -0.0397 & 0.1912 & -0.5428 & 0.7365 & -0.2974 & 0 \\ -0.0081 & -0.0554 & 0.1217 & -0.2974 & 0.2634 & 0 \\ 0 & 0 & 0 & 0 & 0 & 0 \end{bmatrix} *10^5$
Modal frequency before isolated **f** (Hz)	$[0.86\ 2.89\ 5.76\ 9.41\ 12.79]^T$
Modal damping factor before isolated ξ (%)	$[3.00\ 3.00\ 3.00\ 4.90\ 6.66]^T$
Modal frequency after isolated **f** (Hz)	$[0.45\ 1.58\ 3.51\ 6.42\ 10.05\ 13.14]^T$
Modal damping factor after isolated ξ (%)	$[0.33\ 4.10\ 3.96\ 3.67\ 3.58\ 6.90]^T$

$$X(f)=\mathbf{D}(\mathbf{I}-e^{-j2\pi f\Delta t}\mathbf{A})^{-1}(e^{-j2\pi f\Delta t}\mathbf{E}_0+\mathbf{E}_1) \quad \text{(A9)}$$

where $\mathbf{D}=[1\ 0]$ is the location vector of the displacement.

By employing the Newmark method with $\delta=1/2$ and $\alpha=1/4$, the displacement frequency response functions for $\Delta t/T_n=0.1$ and 0.2 are depicted in Fig. A1, while the analytical solution is comparatively presented. When $\Delta t/T_n=0.1$, the peak of the frequency response is slightly reduced in magnitude and shifted leftward, implying a distortion on the dynamic characteristics of the system. In addition, the peak shifts further as $\Delta t/T_n$ increases to 0.2. However, the SSP method indicates no distortion on the frequency response function, even if $\Delta t/T_n=0.2$, as demonstrated in Fig. A2. This observation confirms a complete conservation of the structure's dynamic characteristics employing the SSP method.

Appendix B. Parameters of a multi-story sliding structure

Table 1

References

[1] Buckle IG, Mayes RL. Seismic isolation history: application and performance — a world review. Earthquake Spectra 1990;6:161–201.

[2] Zayas V, Low SS, Main SA. The FPS earthquake resisting system, experimental report. Report no. UCB/EERC-87/01, Earthquake Engineering Research Center, University of California, Berkeley, CA, June 1987.

[3] Kawamura S, Kitazawa K, Hisano M, Nagashima I. Study of a sliding-type base isolation system–system composition and element properties. In: Proc. 9th WCEE; Tokyo-Kyoto, vol. V, 1988:735–40.

[4] Westermo B, Udwadia F. Periodic response of a sliding oscillator system to harmonic excitation. Earthquake Engng Struct Dyn 1983;11:135–46.

[5] Mostaghel N, Hejazi M, Tanbakuchi J. Response of sliding structures to harmonic support motion. Earthquake Engng Struct Dyn 1983;11:355–66.

[6] Mostaghel N, Tanbakuchi J. Response of sliding structures to earthquake support motion. Earthquake Engng Struct Dyn 1983;11:729–48.

[7] Yang YB, Lee TY, Tsai LC. Response of multi-degree-of-freedom structure with sliding supports. Earthquake Engng Struct Dyn 1990;19:739–52.

[8] Nagarajaiah S, Reinhorn AM, Constantinou MC. Nonlinear dynamic analysis of 3-D-base-isolated structures. J Struct Engng, ASCE 1990;117(7):2035–54.

[9] Sues RH, Mau ST, Wen YK. System identification of degrading hysteretic restoring forces. J Engng Mech, ASCE 1988;114(5):833–46.

[10] Rosenbrock HH. Some general implicit processes for the numerical solution of differential equations. Comput J 1964;18(1):50–64.

[11] Lopez-Almansa F, Barbat AH, Rodellar J. SSP algorithm for linear and nonlinear dynamic response simulation. Int J Numerical Meth Engng 1988;26:2687–706.

[12] Mokha AS, Constantinou MC, Reinhorn AM. Teflon bearing in base isolation. I: Testing. J Struct Engng, ASCE 1990;116(2):438–54.

[13] Mokha AS, Constantinou MC, Reinhorn AM. Teflon bearing in base isolation. II: Modeling. J Struct Engng, ASCE 1990;116(2):455–74.

[14] Chopra AK. Dynamics of surfaces — theory and applications to earthquake engineering. Englewood Cliffs, NJ: Prentice-Hall, 1995.